Icarus 277 (2016) 319–329

Contents lists available at ScienceDirect

Icarus

journal homepage: www.elsevier.com/locate/icarus

On the potential for lunar highlands Mg-suite extrusive volcanism and implications concerning crustal evolution

Tabb C. Prissel[a,*], Jennifer L. Whitten[b], Stephen W. Parman[a], James W. Head[a]

[a] Department of Earth, Environmental & Planetary Sciences, Brown University, Providence, RI 02912, United States
[b] Smithsonian Institution, MRC 315, PO Box 37012, Washington, DC 20013-7012, United States

ARTICLE INFO

Article history:
Received 7 November 2015
Revised 5 May 2016
Accepted 8 May 2016
Available online 18 May 2016

Keywords:
Moon
Volcanism
Geological processes
Spectroscopy

ABSTRACT

The lunar magnesian-suite (Mg-suite) was produced during the earliest periods of magmatic activity on the Moon. Based on the cumulate textures of the samples and a lack of evidence for Mg-suite extrusives in both the sample and remote sensing databases, several petrogenetic models deduce a predominantly intrusive magmatic history for Mg-suite lithologies. Considering that ~18% of the lunar surface is covered by mare basalt flows, which are substantially higher in density than estimated Mg-suite magmas (~2900 versus ~2700 kg/m^3), the apparent absence of low-density Mg-suite volcanics is surprising. Were Mg-suite magmas predominantly intrusive, or have their extrusive equivalents been covered by subsequent impact ejecta and/or later stage volcanism? If Mg-suite magmas were predominantly intrusive, what prevented these melts from erupting? Or, if they are present as extrusives, what regions of the Moon are most likely to contain Mg-suite volcanic deposits?

This study investigates buoyancy-driven ascent of Mg-suite parental melts and is motivated by recent measurements of crustal density from GRAIL. Mg-suite dunite, troctolite, and spinel anorthosite parental melts (2742, 2699, and 2648 kg/m^3, respectively) are considered, all of which have much lower melt densities relative to mare basalts and picritic glasses. Mg-suite parental melts are more dense than most of the crust and would not be expected to buoyantly erupt. However, about 10% of the lunar crust is greater in density than Mg-suite melts. These areas are primarily within the nearside southern highlands and South Pole-Aitken (SP-A) basin. Mg-suite extrusions and/or shallow intrusions were possible within these regions, assuming crustal density structure at >4.1 Ga was similar to the present day crust. We review evidence for Mg-suite activity within both the southern highlands and SP-A and discuss the implications concerning crustal evolution as well as Mg-suite petrogenesis. Lower crustal densities measured by GRAIL are consistent with the lack of observed Mg-suite extrusives. If Mg-suite extrusive volcanism was prevented by the low density of the crust, it would suggest the lunar crust was fractured shortly after solidification (>4.3 Ga). The thermal- and stress-state of the lunar crust may have also inhibited Mg-suite extrusion.

1. Introduction

The lunar highlands magnesian-suite (Mg-suite) samples are dominated by igneous, plutonic clasts (dunites, troctolites, norites, and gabbronorites) containing primitive (MgO-rich) mafic silicates and calcic-plagioclase (e.g., James 1980; Papike et al., 1998; Shearer et al., 2015). The positive correlation between MgO-content of mafic silicates and CaO-content of plagioclase within the Mg-suite suggests that the plutonic rocks are related by low-pressure (<0.3 GPa) crystallization from a common parental magma (e.g., Walker et al., 1976; James 1980; Warren 1986; Shearer and Papike 2005). In particular, the forsteritic olivine (forsterite #, or Fo# = Mg/[Mg+Fe] × 100 = Mg#) within the lunar dunites and troctolites (e.g., PST 2003, Fo# ~96 olivine, Snyder et al., 1999) constrain the Mg-suite parental melt to Mg# ≥ 86, which would be the least fractionated melt from the lunar mantle (e.g., Warren 1986; Hess 1994; Longhi et al., 2010; Shearer et al., 2015; Prissel et al.,2016). On the other hand, many of the collected Mg-suite samples contain a KREEP signature (elevated abundances of K-potassium, REE-rare earth elements, and P-phosphorus), suggesting crystallization from an evolved magma (e.g., Hess 1994; Longhi et al., 2010; Shearer et al., 2015). However, KREEP-poor Mg-suite clasts (e.g., dunite 72415 and meteorite Dhofar 489) (e.g., Papike

* Corresponding author.
E-mail address: tcprissel@gmail.com, tabb_prissel@alumni.brown.edu (T.C. Prissel).

http://dx.doi.org/10.1016/j.icarus.2016.05.018
0019-1035/

et al., 1998; Tekada et al., 2006; Gross and Treiman 2011) may indicate that KREEP is not a necessary component of the Mg-suite, and instead reflects sampling near the Procellerum KREEP terrane (PKT) (e.g., Lucey and Cahill 2009; Cahill et al., 2009; Taylor 2009; Prissel et al., 2014a; Shearer et al., 2015). Regardless, Mg-suite plutonic rocks are among the most ancient lunar samples, dating to ~4.3 Ga (e.g., Nyquist and Shih 1992; Borg et al., 2013; Carlson et al., 2014). Thus, ancient ages and primitive major mineralogy indicate that Mg-suite samples can provide insight into the early lunar interior and magmatic activity post-dating the differentiation of a global lunar magma ocean (LMO) (e.g., Wood et al., 1970; Norman and Ryder 1979; James 1980; Hess 1994; Shearer et al., 2006, 2015).

Petrogenetic models use the predominance of plutonic clasts and cumulate textures of the Mg-suite samples to suggest parental magmas formed intrusions within the anorthositic crust, implying they did not erupt (e.g., James 1980; Warren 1986; Hess 1994; Longhi et al., 2010; Shearer et al., 2015). Indeed, few extrusive clasts are chemically similar to the plutonic Mg-suite dunites and troctolites, consistent with current petrogenetic models (e.g., 73215,170, James and Hedenquist 1978; Jessberger et al., 1979; 14305, Arai et al., 2006; ALHA 81005, Treiman and Gross, 2013, 2015). Additionally, visible and near-infrared (V-NIR) remote sensing data have found no clear evidence for ancient, Mg-suite volcanic deposits (Prissel et al., 2013, 2015).

Density estimates for Mg-suite parental magmas are substantially lower than mare basalts and picritic glasses (Prissel et al., 2013, 2015). Thus, the lack of a low-density, extrusive equivalent to the ancient Mg-suite dunites and troctolites is surprising considering that dense mare basalts and picritic melts have erupted to cover ~18% of the lunar surface (e.g., Head 1976; Head and Wilson 1992; Rutherford and Papale 2009; Whitten and Head 2015a; Sori et al., 2016). It is possible that the younger mare basalt flows have buried ancient, Mg-suite eruptions. However, the ancient and intrusive Mg-suite samples were recovered despite a prolonged history of volcanic activity on the Moon.

Earlier studies (e.g., Snyder et al., 1995a, 1995b; Papike et al., 1996) suggested that the younger (3.8–4.08 Ga) lunar KREEP basalts could represent an extrusive equivalent to the ancient (~4.3 Ga), plutonic Mg-suite norites and gabbronorites and/or the evolved highlands Alkali-suite rocks (Warren 1988; Nyquist and Shih 1992; Ryder 1994; Hess 1995; Hess and Parmentier 1995; Papike et al., 1998; Shearer and Papike 1999; Shearer et al., 2006; Carlson et al., 2014). First, the distinct ages between the Mg-suite plutonic rocks and KREEP basalts imply the two are unrelated, though the age gap could be the result of an unrepresentative sample collection (e.g., Nyquist and Shih 1992; Shearer et al., 2006; Borg et al., 2013; Carlson et al., 2014; Shearer et al., 2015). Nevertheless, several additional factors indicate the ancient plutonic Mg-suite rocks are distinct from younger episodes of KREEP basaltic volcanism including: 1) major mineralogy of the olivine-absent KREEP basalts is much more evolved than the olivine-essential dunites and troctolites of the Mg-suite (e.g., KREEP basalt Mg# < 66; dunite and troctolite parent Mg# > 86), 2) Mg-suite apatite is enriched in Cl relative to both mare basalts and KREEP basalts, and 3) the KREEP-poor Mg-suite-like clasts in meteorite Dhofar 489 imply KREEP is not a necessary petrogenetic component of the Mg-suite (see Shearer et al., 2015 and references therein for further discussion). Assuming a conclusive chemical connection between KREEP basalts and the Mg-suite is determined, the evolved mineralogy of KREEP basalts would then indicate they represent a highly fractionated, residual daughter liquid of melts parental to the primitive Mg-suite troctolites and dunites, regardless of origin.

If the ancient and primitive Mg-suite parental magmas were predominantly intrusive, as the current sample set and petrogenetic models imply, what prevented low-density Mg-suite parental melts from erupting? Or, if they are present as extrusive deposits, what regions of the Moon are most likely to contain evidence for primitive Mg-suite volcanism? The present study is motivated by updated crustal densities from NASA's Gravity Recovery and Interior Laboratory (GRAIL) mission and explores the potential for ancient, Mg-suite extrusive volcanism as well as what regions of the Moon, if any, were conducive to Mg-suite volcanic activity.

1.1. Premise

Crustal density plays a major role in determining whether or not magmas erupt because buoyancy forces (i.e. the density contrast between melt and wallrock) primarily control melt transport (e.g. Solomon 1975; Wilson and Head 1981; Delano 1990; Lister and Kerr 1991; Rubin 1995; Wieczorek et al., 2001; Michaut 2011; Prissel et al., 2013). In buoyancy-driven magmatic ascent, magmas will rise through source material until reaching a layer of equal or lesser density, such as a crust-mantle interface. This layer is called the level of neutral buoyancy (LNB). Thus, low crustal densities will act to limit or prevent eruption of magmas.

Recent estimates of bulk crustal density by NASA's GRAIL mission are considerably lower (~2550 kg/m^3) than previous estimates (~2890 kg/m^3) (Wieczorek et al., 2013). The low values are inferred to be the result of high porosities throughout the lunar crust (4–21%) (e.g., Wieczorek et al., 2013; Besserer et al., 2014; Han et al., 2014). This finding suggests that the long history of impacts on the Moon has brecciated the crust from top to bottom. If the ancient lunar crust (> 4.1 Ga) was brecciated and low-density as it is today, it may explain why Mg-suite magmas did not erupt. Likewise, the absence of Mg-suite extrusive deposits could be evidence that the crust was strongly fractured (i.e., low-density) early in lunar history.

To test this hypothesis, we investigate buoyancy-driven magmatic ascent of Mg-suite parental melts. Melt densities are calculated for a range of theoretical Mg-suite parental magmas. Results are compared with GRAIL data to delineate regions of the Moon where Mg-suite melts are less dense than the present day lunar crust (i.e., areas that could have allowed for Mg-suite eruptions). Only a small percentage of the current lunar crust is of greater density than Mg-suite magmas. These potential regions of eruption are reviewed for evidence of ancient Mg-suite volcanic activity.

2. Methods and data

2.1. Mg-suite parental melt compositions

The Mg-suite parental melt must be inferred from known intrusive lithologies (Longhi et al., 2010). However, few major element estimates of the Mg-suite parental melt have been made (Warren 1986; Longhi et al., 2010; Sonzogni and Treiman 2015; Prissel et al., 2016). Melt inclusions within Mg-suite norite samples (Sonzogni and Treiman, 2015) are not well suited here as they represent an evolved or residual component of the Mg-suite parent (James 1980; Warren 1986; Hess 1994; Carlson et al., 2014). The lunar dunites and troctolites on the other hand, are among the most primitive samples within the Mg-suite and are the most common basis for constraining the Mg# and bulk composition of the Mg-suite parental melt (e.g. Warren 1986; Ryder 1991; Hess 1994; Longhi et al., 2010; Elardo et al., 2011; Shearer et al., 2015; Prissel et al., 2016).

Three Mg-suite lithologies are used to test a range of possible Mg-suite parental melts: the Mg-suite troctolites, dunites, and remotely detected pink spinel anorthosites (PSA). The compositions, Mg#, and liquidus temperatures of all three theoretical Mg-suite parental magmas are reported in Table 1.

Longhi et al. (2010) provides an estimate of the lunar troctolite parental melt, which is in equilibrium with Fo# = 95 olivine. The

Table 1
Starting compositions considered in this study.

	Dunite parent[a]	Troctolite parent[b]	PSA parent[c]
SiO_2	45.90	45.40	44.56
TiO_2	1.58	0.96	0.47
Al_2O_3	6.49	17.89	26.50
Cr_2O_3	0.61	0.37	0.16
FeO	7.91	4.89	2.61
MnO	0.35	0.22	0.07
MgO	28.41	17.24	8.83
CaO	7.46	12.15	16.46
Na_2O	0.49	0.41	0.19
K_2O	0.79	0.48	0.15
Total	100	100	100
Mg#	87	87	87
Liq T °C	1554	1381	1375

Mg# = cation fraction of [Mg/(Mg + Fe)] × 100.
Liq T °C = liquidus temperature.
[a] Prissel et al. (2016).
[b] Longhi et al. (2010).
[c] Prissel et al. (2014).

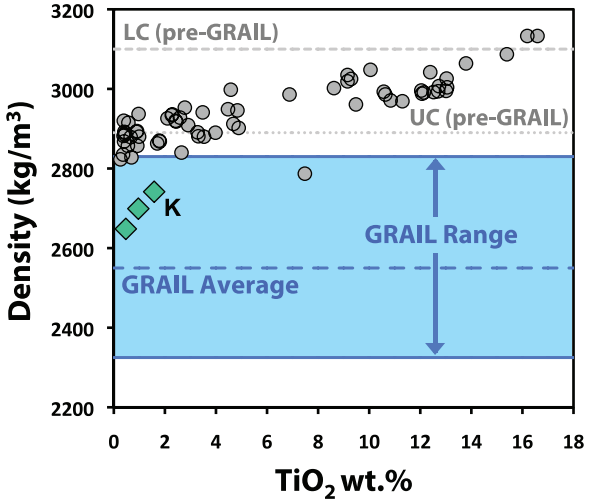

Fig. 1. 1-atm melt density of lunar basaltic compositions as a function of TiO_2 content in the melt (similar to Finnila et al., 1994 and Wieczorek et al., 2001). Shown for reference are the pre-GRAIL estimates of lower (LC) and upper crustal (UC) density (grey dashed and dotted lines, respectively; Wieczorek et al. (2013)) as well as updated estimates from GRAIL (density range denoted by blue-field, with average density represented by dashed blue line; Wieczorek et al., 2013). Gray-filled circles represent mare basalt and picritic glass compositions (Papike et al., 1976; Delano 1986; Wieczorek et al., 2001). Teal-filled diamonds represent a range of Mg-suite parental melt densities. "K" represents KREEP basalt 15386 (Prissel et al., 2013). Lower average crustal densities from GRAIL appear necessary in order to have prevented ancient, Mg-suite magmas from erupting to the surface. (For interpretation of the references to color in this figure legend, the reader is referred to the web version of this article.)

Mg# of Longhi et al. (2010) parental melt (≥ 86) is used here to constrain the Mg# of alternative theoretical compositions since the Mg-suite is thought to be derived from a common source (James, 1980; Warren, 1986; Carlson et al., 2014).

The Mg-suite dunites (e.g., samples 72415, 72416, 72417, and 72418) are also considered in our model. Because the dunites contain little to no feldspar and are comprised of olivine similar in composition to the lunar troctolites (e.g. Ryder 1991; Shearer et al., 2012, 2015), they likely represent the product of a plagioclase-undersaturated Mg-suite parental melt (e.g., Warren 1986; Prissel et al., 2015, 2016). Dunites also contain trace amounts of chromite and thus, plagioclase-undersaturated melts in equilibrium with chromite are used for our hypothesized Mg-suite dunite parent (Prissel et al., 2016).

The pink spinel anorthosites (PSA) are remotely detected outcrops dominated by anorthitic feldspar and Mg-spinel ($MgAl_2O_4$), or pink spinel (e.g. Pieters et al., 2011; Dhingra et al., 2011). Mg-spinel is rare among the lunar samples and most commonly associated with the pink spinel troctolites (PST) of the Mg-suite (Prissel et al., 2014, 2016). Unlike the PST of the Mg-suite however, PSA detections show no spectral evidence for olivine ± pyroxene. The high Mg# and low Cr# interpreted for PSA spinel (e.g. Pieters et al., 2011; Jackson et al., 2014; Williams et al., 2012, 2016), as well as the lack of a mafic spectral signature, suggests PSA parental melts contained spinel and plagioclase as primary liquidus phases. In order to explain PSA spinel compositions and the lack of a mafic silicate phase, Prissel et al. (2014) experimentally determined that PSA parental melts must be similar to Mg-suite parental melts in Mg# ≥ 86, but require a higher normative anorthite component relative to melts parental to the lunar troctolites. Based on these criteria, the PSA parental melt is estimated by adding normative anorthite to the Mg-suite troctolite parent melt while holding Mg# constant. The normative anorthite content of the experimental melts produced in Prissel et al. (2014) serve as a proxy for our theoretical PSA parental melt (Table 1).

2.2. Viscosity considerations and calculation of melt density

In addition to buoyancy-driven magmatic ascent, the viscosity contrast between intruding magmas and the host rock can also dictate whether ascending melts form dikes or intrusions (e.g., Rubin 1993, 1995). For instance, a low viscosity contrast can exist between viscous granitic magmas and the host rock, which promotes diapiric, intrusive magmatic behavior (e.g. Huppert and Sparks, 1988; Rubin, 1993). We have calculated the viscosities of the three Mg-suite compositions above, a range of picritic glasses, and also the high- and low-Ti mare basalts using the methods of Shaw 1972 (Supplementary Fig. 1). Considering the Mg-suite compositions investigated above, viscosity increases with the incorporation of a normative anorthite component because Al_2O_3 acts as a network-former and –modifier in silicate melts (e.g., Bottinga and Weill, 1972; Shaw, 1972). Regardless of their Al_2O_3 content however, all Mg-suite parental melts investigated are similar in viscosity to other lunar basaltic samples, nearly four orders of magnitude less viscous than granitic magmas (Supplementary Fig. 1) (e.g., Taylor and Lu, 1992). Thus, a low viscosity contrast between Mg-suite parental melts and the lunar crust is unexpected (Supplementary Fig. 1). Here, we assume buoyancy-driven magmatic ascent primarily controls Mg-suite melt transport.

The 1-atm liquidus densities of Mg-suite parental melts are calculated using the methods of Lange and Carmichael (1990). To compare Mg-suite melt densities with known lunar basaltic compositions, the 1-atm liquidus densities of mare basalts (Papike et al., 1976), pictritic glasses (Delano, 1986), and KREEP basalt 15386 (Papike et al., 1998; Prissel et al., 2013) are also calculated using the same methods as above (Fig. 1). Here, the partial molar volumes of MnO and Cr_2O_3 are estimated by using the partial molar volumes of FeO and Fe_2O_3, respectively. The ionic radii ratio of both Mn/Fe^{2+} and Cr/Fe^{3+} is ~1 (Shannon and Prewitt, 1969), thus the partial molar volumes of the respective oxides are analogous to one another. Because MnO and Cr_2O_3 are minor components in most lunar basaltic systems, our 1-atm liquidus densities are comparable to those calculated by Wieczorek et al. (2001) (Table 2).

For simplicity, all compositions are assumed to be anhydrous. Xu et al. (2014) examined the effects of dissolved water in the eruptibility of the picritic glasses, incorporating a range between 1000 and 5000 ppm H_2O in their eruption model. Note however, the lowest estimates used in Xu et al. (2014) appear to be maxima for dissolved water in the lunar glasses (see Saal et al., 2008; Hauri et al., 2015). Regardless, the addition of ~0.10 wt% H_2O decreases

Table 2
1-atm Melt densities with the effects of pressure and water.

Mg-suite data	T °C	Density (kg/m^3)		2 kbar
Dunite parent	1554	–	2742	2766
Troctolite parent	1381	–	2699	2725
PSA parent	1375	–	2648	2675
KREEP basalt data				
	Rutherford et al., 1996		Present study	
	Liq T °C	Density (kg/m^3)		+0.10 wt% H_2O
15386	1180	–	2703	2696
Volcanic glass data				
Delano (1986)	Wieczorek et al. (2001)		Present study	
VLT glasses	Liq T °C	Density (kg/m^3)		+0.10 wt% H_2O
1	1406	2827	2823	2814
2	1402	2886	2882	2872
3	1406	2923	2920	2910
4	1399	2871	2868	2858
5	1411	2896	2892	2882
6	1422	2889	2885	2875
7	1435	2893	2889	2879
8	1371	2861	2857	2848
9	1408	2918	2915	2904
10	1358	2881	2879	2869
11	1446	2895	2894	2884
12	1403	2941	2937	2927
Low-Ti glasses				
13	1338	2945	2941	2931
14	1373	3001	2998	2987
High-Ti glasses				
15	1316	2990	2986	2975
16	1358	3006	3002	2991
17	1366	3024	3019	3008
18	1369	3040	3035	3024
19	1294	3029	3025	3014
20	1357	3053	3048	3037
21	1349	3049	3042	3031
22	1298	3069	3064	3053
23	1322	3087	3087	3076
24	1326	3140	3133	3122
25	1326	3140	3133	3122
Mare basalt data				
	Wieczorek et al. (2001)		Present study	
Mare basalts	Liq T °C	Density (kg/m^3)		+0.10 wt% H_2O
VLT/high-Al				
70008	1272	2839	2835	2826
24109	1164	2893	2892	2884
VLT/low-Al				
70007	1289	2832	2828	2819
78526	1302	2862	2857	2848
Low-Ti/high-Al				
24182	1169	2881	2880	2872
14053	1202	2841	2840	2832
Luna 16, B1	1173	2904	2902	2894
Low-Ti/low-Al				
15058	1237	2867	2863	2854
15499	1239	2873	2870	2861
15597	1224	2871	2868	2859
15555	1300	2931	2926	2917
15016	1301	2942	2936	2927
12035	1383	2938	2934	2924
15545	1272	2925	2920	2911
12040	1395	2922	2918	2908
12002	1369	2935	2928	2918
12005	1466	2959	2953	2943
12009	1296	2912	2909	2899
12052	1208	2894	2891	2882
12011	1208	2885	2881	2872
12021	1180	2882	2880	2872
12064	1157	2898	2890	2881
12008	1317	2953	2949	2939

(*continued on next page*)

Table 2
(*continued*)

Mare basalts	Liq T °C	Density (kg/m^3)		+0.10 wt% H_2O
12051	1172	2917	2912	2903
12022	1284	2950	2946	2937
High-Ti/high-Al				
14063	1114	2788	2787	2779
High-Ti/low-Al				
10047	1119	2962	2961	2952
10003	1156	2995	2993	2984
10020	1187	2989	2986	2977
75055	1154	2972	2971	2962
10049	1156	2971	2969	2959
70275	1129	2997	2996	2987
74245	1230	2991	2988	2978
10072	1183	2993	2991	2981
74255	1252	2996	2992	2982
76136	1204	3010	3007	2998
74275	1244	2998	2994	2984
70035	1236	3008	3004	2994
70215	1201	3028	3026	3016
70017	1235	2998	2995	2845

T °C = liquidus *T* calculated by Prissel et al. (2016) and Longhi et al. (2010).
Liq T °C = liquidus temperature calculated by Rutherford et al. (1996) and Wieczorek et al. (2001).
VLT = very low-Ti glasses.

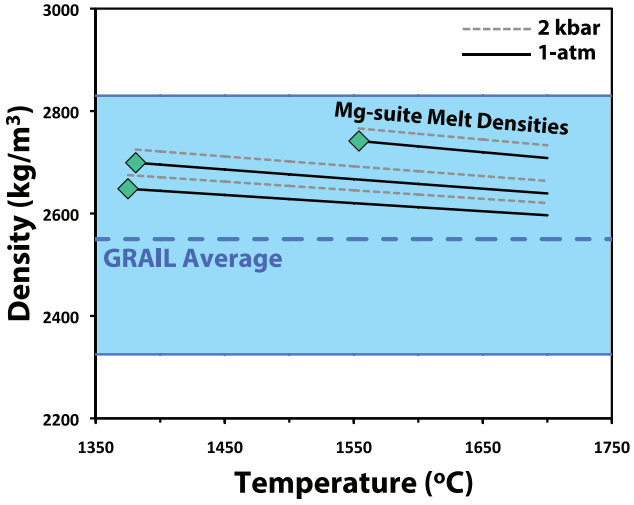

Fig. 2. The range of calculated 1-atm and 2 kbar Mg-suite melt densities vs. temperature of the melts (horizontal solid-black and dashed-grey lines, respectively). The range of crustal densities from GRAIL are denoted by the blue-field, with average density represented by the horizontal, dashed-blue line. The general effects of temperature over a large interval (respective liquidus temperatures to 1700 °C) are shown. Relative to melt densities, the effects of temperature on crustal density are negligible and thus, not shown here. (For interpretation of the references to color in this figure legend, the reader is referred to the web version of this article.)

the melt density by only ~10 kg/m^3 (Xu et al., 2014), a small effect (Table 2).

Both temperature and pressure affect the density of basaltic melts (e.g. Lange and Carmichael, 1987,1990; Kress and Carmichael, 1991; Ghiorso and Kress, 2004). The effect of temperature on Mg-suite parental melt density is shown for reference (Fig. 2). The most recent estimates of lunar crustal thickness (Wieczorek et al., 2013) report an average of 34–43 km. The upper average value of 43 km corresponds to ~2 kbar pressure on the Moon. Mg-suite melt densities at this pressure are also calculated for comparison (Table 2, Fig. 2).

2.3. Global average crustal density and criteria for identifying potential regions of Mg-suite eruptions

We assume that current crustal densities measured by GRAIL can be applied to the ancient lunar crust at the time of Mg-suite magmatism (> 4.1 Ga) (e.g. Nyquist and Shih, 1992; Carlson et al., 2014). If, however, crustal densities were higher due to factors such as less impact fracturing, magmas would be more likely to erupt (Fig. 1). Only highland regions of the crust are considered for this analysis. Regions of the crust with exposed mare basalts are not included (gray-filled regions in Fig. 3); any ancient extrusive deposits in these areas would be undetectable as they are covered by younger mare basalt flows.

The porous megaregolith is predicted to extend to depths of ~10–20 km within the lunar crust (e.g., Han et al., 2014). Below these depths, porosity closes due to lithostatic overburden and crustal density is estimated to be closer to solid anorthosite (2800–2900 kg/m^3) suggesting a stratified lunar crust (e.g., Han et al., 2014). The increase in crustal density (i.e., decrease in porosity) with depth could also be the result of thermal evolution/viscous deformation (e.g., Besserer et al., 2014). Regardless, the lowest crustal density impeding extrusive volcanism exists within the porous, near-surface megaregolith (pressures ~0.05 GPa). Because melt density does not significantly change within the pressure range of the lunar crust (Table 2), 1-atm Mg-suite melt densities are used to compare to the near-surface, porous crustal densities from GRAIL.

Average global crustal density maps are produced from GRAIL crustal density models with an average crustal thickness of 34 km, a minimum thickness of 0.6 km, a crustal porosity of 12%, and a mantle density of 3220 kg/m^3 (Wieczorek et al., 2013). The data were interpolated to create a raster of average global crustal density (ignoring the boundary conditions at 0/360° longitude). Similar to the mare eruption model of Wieczorek et al. (2001), buoyancy-driven magmatic ascent on the Moon is investigated with Mg-suite parental melts (Prissel et al., 2013, 2015). Potential regions of Mg-suite eruptions are defined as the areas where the 1-atm melt densities are less than near-surface crustal densities. The potential areas of eruption predicted here do not suggest volcanism has occurred. Instead, highlighted regions only im-

ply that eruptions are possible assuming Mg-suite melts were present.

3. Results

3.1. Mg-suite parental melt density

All melt densities, including picritic glasses, mare basalts, and KREEP basalt for comparison, are reported in Table 2 and plotted in Fig. 1. The Mg-suite dunite, troctolite, and PSA parental melt 1-atm liquidus densities are 2742, 2699, and 2648 kg/m^3, respectively. Melt density positively correlates with TiO_2 and FeO content due to their high molecular weights (as can be seen with the mare basalts and picritic glasses, see also Finnila et al., 1994; Wieczorek et al., 2001). Thus, the low TiO_2 and FeO contents of Mg-suite parental melts contribute to their low densities (Fig. 1). At similar TiO_2 content, the higher Mg# composition will have a lower density because the molecular weight of FeO > MgO. Incorporation of anorthite decreases the density of mafic melts due to the large molar volume of Al_2O_3 (Lange and Carmichael, 1990). Melt density also decreases with temperature owing to the thermal expansion of the oxide components (Fig. 2). Conversely, melt density increases with pressure because liquids are highly compressible. However, because of the Moon's low gravity, crustal pressures are low (< 2 kbar) and have minimal effect on Mg-suite melt density (Table 2).

3.2. Potential regions of Mg-suite extrusive volcanism

Using the buoyancy model described above and the updated crustal density measurements from GRAIL, Mg-suite parental melts are less dense than only a small portion (<10%) of the Moon's crust (Fig. 3). The highest density Mg-suite melt investigated is the plagioclase-undersaturated melt (2742 kg/m^3). Comparing with crustal densities from GRAIL, the plagioclase-undersaturated melt results in the fewest potential eruptive regions, which are predominantly restricted to the South Pole-Aitken basin (SP-A) (Fig. 3a). In addition to regions within SP-A, the Mg-suite troctolite parent melt (2699 kg/m^3) is capable of erupting within a few small regions of the southern highlands (Fig. 3b). Our Mg-suite PSA melt has the lowest density of the three melts considered (2648 kg/m^3) and is therefore associated with the largest area of potential eruptive regions, which are present on both the lunar nearside and farside (Fig. 3c).

4. Discussion

Results from this study suggest only a small percentage (<10%) of the lunar surface contain potential localities for ancient, Mg-suite eruptions (black-filled regions in Fig. 3). All Mg-suite parental melt densities calculated in this study plot within the range of crustal densities measured by GRAIL (Fig. 1). The Mg-suite plagioclase-undersaturated melt (2742 kg/m^3) is most likely to remain intrusive relative to the other Mg-suite melts considered because it is less dense than the lunar crust (2830 kg/m^3) only within SP-A (Fig. 3a). The paucity of potential eruptive regions predicted for the Mg-suite plagioclase-undersaturated parental magma is consistent with the current sample set and petrogenetic models, which imply Mg-suite magmas were predominantly intrusive (e.g. James, 1980; Warren, 1986; Shearer and Papike, 2005; Longhi et al., 2010; Elardo et al., 2011).

The buoyancy model indicates a few potential areas of eruption for the troctolitic and PSA parent melts, however (Fig. 3b,c). The relatively lower densities of the troctolitic and PSA melts (2699 and 2648 kg/m^3, respectively) compared to the plagioclase-undersaturated melt result in a greater total area of potential eruptive regions focused primarily within the nearside southern highlands and SP-A. Below, we review remote sensing evidence for Mg-suite lithologies within the predicted areas of eruption concentrated within the nearside southern highlands and SP-A basin.

4.1. Remote sensing evidence for Mg-suite and correlations with predicted eruptive regions

If Mg-suite volcanic deposits are present in an area, it is likely that Mg-suite intrusions will also be present and thus, may have been exposed or excavated by impacts. While there is no clear spectral evidence for Mg-suite extrusive deposits, there is evidence for exposed Mg-suite intrusions. Correlations between the potential Mg-suite eruption sites identified above and published locations of Mg-suite related rocks, such as Mg-spinel anorthosites, are investigated below.

Remote sensing methods have been used to identify intrusive lithologies exposed at the central peaks or basin walls of impact structures (e.g. Tompkins and Pieters, 1999; Pieters et al., 2011; Dhingra et al., 2011; Yamamoto et al., 2012a; Pieters et al., 2014). While the relative abundance of minerals can be inferred from the spectral data (e.g., Cheek and Pieters 2014), characterizing the Mg# of mafic silicates, a distinguishing characteristic of the Mg-suite, is challenging. More recently however, the identification of a potentially new lunar rock type, pink spinel anorthosite (PSA) (Pieters et al., 2011; Dhingra et al., 2011), may provide a robust method in identifying Mg-suite lithologies remotely (e.g., Jackson et al., 2014; Prissel et al., 2014, 2016; Williams et al., 2016). A strong compositional link was found between Mg-suite melts and PSA spinel compositions in the experimental study of Prissel et al. (2014). If true, remotely detected outcrops of PSA can be used as a proxy for Mg-suite activity on the Moon (Prissel et al., 2014).

4.1.1. Nearside southern highlands

Plotted in Fig. 3c are the global locations of PSA detections from Pieters et al. (2014). Among the 23 total PSA detections shown, 15 are within the lunar highlands region considered for this study; the remaining 8 are located in the Procellarum KREEP Terrane (PKT) or mare filled basins not considered in our analysis. Of those 15 PSA detections, 10 are located in the nearside southern highlands region of the Moon. Remotely detected PSA are interpreted to be intrusive lithologies that have been exposed and excavated by impacts (e.g., Pieters et al., 2011; Dhingra et al., 2011; Gross and Treiman 2011; Pieters et al., 2014). If PSA can be used as a proxy for Mg-suite activity (Prissel et al., 2014), the nearside southern highlands region of the Moon appears to contain a widespread network of Mg-suite intrusions. Thus, the strong correlation of PSA near the predicted eruptive regions in the nearside southern highlands suggests this is the most promising region to search for both ancient intrusions and volcanic deposits of the lunar highlands Mg-suite.

For example, a recent investigation (Sori et al., 2016) combining gravity data from GRAIL (e.g., Wieczorek et al., 2013) and topography data from the Lunar Orbiter Laser Altimeter instrument aboard the Lunar Reconnaissance Orbiter (Chin et al., 2007; Smith et al., 2010) has identified a large arc of positive Bouguer anomolies spanning the southern highlands region of the lunar nearside. The large southern-arc of positive Bouguer anomolies identified by Sori et al. (2016) is interpreted to be a network of buried mafic intrusions and/or extrusives (possibly Mg-suite), and is centered over the candidate Mg-suite eruptive regions predicted here (Fig. 3c). As will be discussed in the following section, it is clear that low-density, low-FeO Mg-suite compositions should be considered (in addition to high-density, high-FeO mare compositions) in future remote sensing studies of volcanic and magmatic activity in the nearside southern highlands region of the Moon.

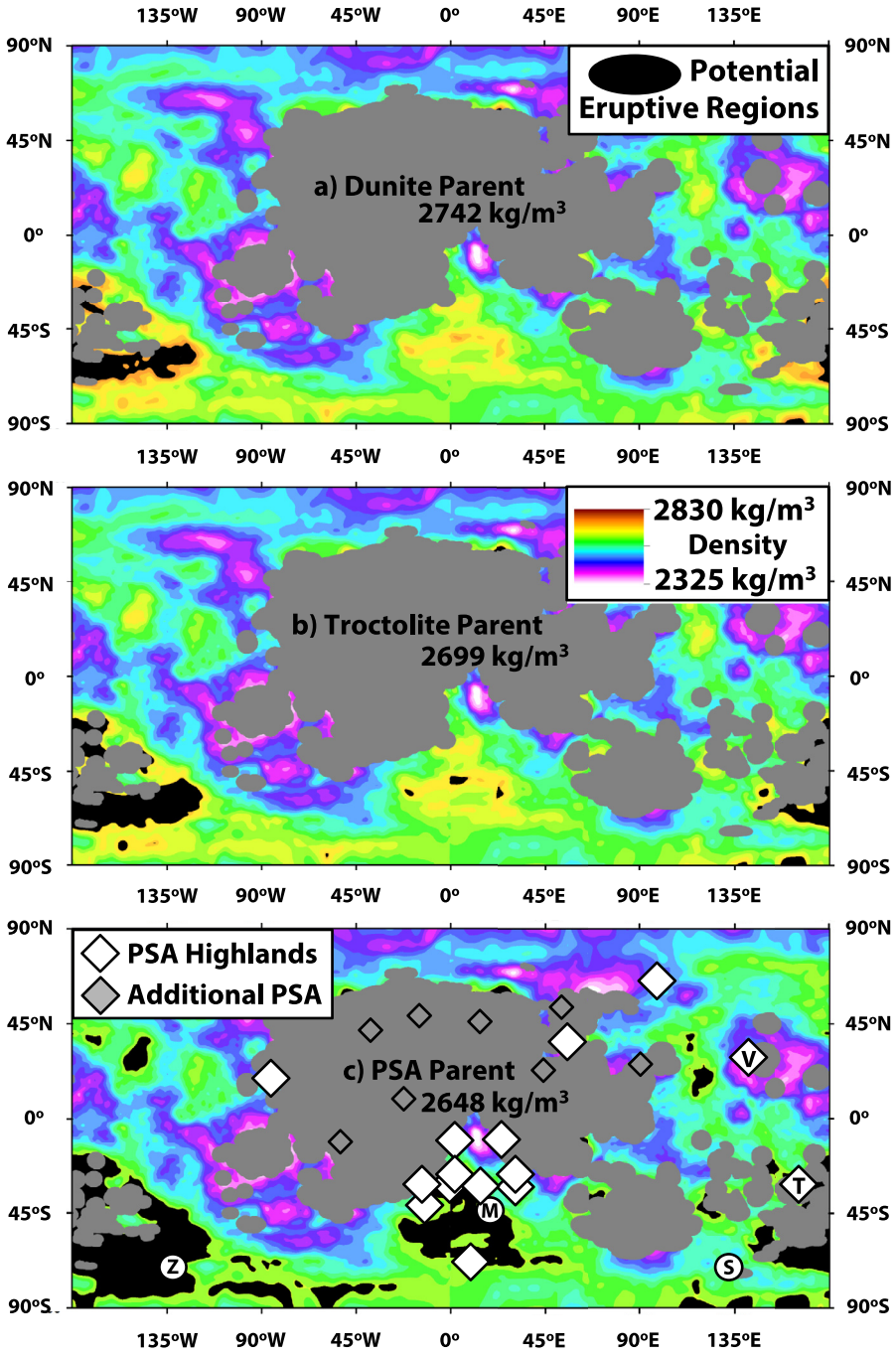

Fig. 3. Global average crustal density from GRAIL shown in color scale (legend in plot b, see text for model parameters) with areas of potential Mg-suite extrusion (black-filled regions). Grey-filled mare basalt regions were not considered in this study (see text for explanation). Melt densities are provided in each plot. a) The 1-atm Mg-suite plagioclase-undersaturated melt density compared to GRAIL crustal densities. b) The troctolite parent melt is less dense than the plagioclase-undersaturated Mg-suite composition and results in regions for potential eruption in the nearside southern highlands in addition to the SP-A basin. c) PSA parental melt with the greatest overall potential area for eruption within the nearside southern highlands and SP-A basin. Diamonds are PSA detections (Pieters et al., 2014), white-filled diamonds plot within areas considered in this analysis whereas grey-filled diamonds plot within mare-filled regions not analyzed. PSA detections at Moscoviense Basin and Thomson crater (whit-filled diamonds labeled with "V" and "T," respectively) are labeled for reference, as are the Low-FeO igneous deposits at Maurolycus and olivine-rich exposures within Schrödinger basin and Zeeman crater (white-filled circles labeled "M," "S," and "Z," respectively). The strong correlation of PSA detections (Pieters et al., 2014) with results from this analysis suggests the nearside southern highlands region is the most promising area to search for possible Mg-suite volcanic and intrusive deposits (see text for further discussion). (For interpretation of the references to color in this figure legend, the reader is referred to the web version of this article.)

4.1.2. South Pole-Aitken basin

PSA is detected at Thomson crater in SP-A and the remaining four PSA locations are not correlated with any of the predicted eruptive regions (Fig. 3c). The Mg-spinel exposures at Thomson crater are presently the most extensive of any PSA detection (Pieters et al., 2014). Additionally, olivine-rich exposures are located in the central peaks and rings of Schrödinger basin and Zeeman crater and have been characterized as high-Mg# lithologies (Yamamoto et al., 2012b; Kramer et al., 2013). The detection of both high Mg#, olivine-rich lithologies in Schrödinger basin, Zee-

man crater and extensive Mg-spinel lithologies at Thomson crater supports the presence of high-MgO material (possibly Mg-suite) underlying a small portion of the SP-A floor.

4.1.3. Farside feldspathic highlands

Finally, Mg-suite eruptions are not expected within the farside feldspathic highlands region of the Moon (Fig. 3c). Additionally, the low number of PSA detections within this region may indicate that Mg-suite magmatism was not as prevalent on the lunar farside as it perhaps was within the PKT or nearside southern highlands (e.g., Haskin et al., 2000; Jolliff et al., 2000; Wieczorek and Phillips, 2000). The possible absence of Mg-suite magmatism on the farside would support remote sensing studies suggesting olivine-rich crustal material is restricted to the nearside lower lunar crust (e.g., Yamamoto et al., 2012b). However, PSA detections are typically associated with areas of thin crust, including Moscoviense basin on the lunar farside (Fig. 3c) (Pieters et al., 2014). Thus, it is possible that deep-seated PSA lithologies within the thick, farside feldspathic highlands crust may not have been excavated. In this case, the absence of PSA and Mg-suite within the farside highlands cannot be used as evidence against their presence.

4.2. Reconsidering Mg-suite deposits in future remote sensing studies

Given the predominance of intrusive Mg-suite samples, the remote identification and characterization of Mg-suite extrusive deposits has not been a primary focus in studies of lunar volcanism. Assuming PSA can be used as a proxy for Mg-suite however, the proximity of several PSA detections within the predicted eruptive region in the southern highlands merits further consideration. For instance, evidence for low-FeO, magmatic activity has been observed in the southern highlands of the lunar nearside, specifically around Maurolycus crater (Scott, 1972; Giguere et al., 1998; Hawke et al., 2002). While the region is largely devoid of volcanic deposits at the surface, several dark-halo impact craters (DHC) and dark rayed craters have been identified (indicating buried mafic material, or "cryptomare") (e.g., Head and Wilson, 1992; Hawke et al., 2002). Yamamoto et al. (2015) also identified the presence of high-Ca pyroxene deposits associated with the cryptomare regions, consistent with possible igneous activity. In particular, dark (low albedo) rays have been observed extending away from crater Maurolycus A (45.3°S, 14.5°E), which may represent the excavation of a buried mafic intrusion (Giguere et al., 1998; Hawke et al., 2002). The FeO concentration associated with the lower albedo rays extending from Maurolycus A is on the order of 5–9 wt% (Hawke et al., 2002). The low-albedo FeO values are similar with the surrounding lighter albedo highlands material (5–11 wt% FeO), but much lower than both local mafic deposits within the region (12–14 wt% FeO) and typical mare basaltic compositions (15–18 wt% FeO). To explain the presence of low albedo, low-FeO dark rays, Hawke et al. (2002) suggest that low albedo mafic material may have mixed with low-FeO highlands material during impact.

While the low-FeO mafic material can be explained by mixing with highlands material, it would also be consistent with low-FeO Mg-suite basaltic compositions reported here (Table 1). Because Mg-suite is ancient, many (if not all) Mg-suite volcanic deposits on the nearside would likely have been buried during the Imbrium impact (Treiman and Gross, 2013) or covered by younger mare basalt flows. If Mg-suite intrusive or extrusive deposits are buried, they could be exposed and identified similar to cryptomare deposits (via the presence of DHC) (e.g. Schultz and Spudis, 1979; Hawke and Bell, 1981; Head and Wilson, 1992; Whitten and Head, 2015a, 2015b). Additionally, Mg-suite intrusions and/or buried volcanic deposits could be identified via positive Bouguer anomolies using gravity and topography data including gravitational signals beneath floor fractured craters (e.g., Jozwiak et al., 2012, 2015; Thorey et al., 2015; Sori et al., 2016). Results from the present analysis suggest low-density, low-FeO Mg-suite material, in addition to typical high-density, high-FeO mare compositions, should be included in future remote sensing studies and geophysical models of ancient lunar volcanic and magmatic activity, particularly in the nearside southern highlands of the Moon.

4.3. Implications concerning crustal evolution and mare volcanism

One of the more intriguing results from this study is that Mg-suite parental melts are ~200–300 kg/m^3 less dense than average mare basalts (Fig. 1). Thus, it is surprising that high-density mare basalts have erupted and cover a significant portion of the lunar surface, but ancient, low-density Mg-suite extrusive deposits have not been observed. As stated above, it is possible that ancient Mg-suite lavas erupted onto the surface, but have since been covered by younger mare basalt flows or destroyed by impacts. Assuming Mg-suite parental magmas were predominantly intrusive, we discuss potential causes for the apparent paradox of ancient, low-density magmatic intrusions and younger, high-density volcanic eruptions.

If GRAIL has measured the present-day porosity of the lunar crust, when did the fracturing occur? Results from this analysis suggest present day, low-crustal densities measured by GRAIL are needed to have prevented ancient, low-density plagioclase-undersaturated Mg-suite parental melts from buoyantly erupting (Fig. 1). Because the Mg-suite samples are ancient (~4.3 Ga) and predominantly intrusive, the results imply the primary lunar crust was fractured soon after solidification perhaps creating a porous, low-density barrier to eruption.

Alternatively, a hotter or partially molten crust has been suggested to explain the presence of large, linear gravity anomalies (interpreted as ancient igneous intrusions) globally distributed across the Moon (Andrews-Hannah et al., 2013). A partially molten or ductile crust would impede early magmatic ascent due to increased lateral plastic deformation during intrusion (Huppert and Sparks, 1988; Rubin, 1993). A hotter or partially molten crust would also be more susceptible to magma-wallrock interactions, which may have led to production of Mg-spinel ($MgAl_2O_4$)-bearing lithologies on the Moon (Morgan et al., 2006; Prissel et al., 2012, 2014, 2016). Thus, the detection or confirmed absences of ancient Mg-suite extrusive deposits can help to further constrain the thermal and stress-state of the ancient lunar crust.

4.3.1. Additional factors controlling magmatic ascent

Younger, high-density mare basaltic volcanism appears to require more than buoyancy forces alone (Fig. 1). For instance, eruption is more likely within regions experiencing extensional stresses (e.g., Lister and Kerr, 1991). Recent GRAIL measurements of rectilinear gravity anomalies bordering the PKT region of the Moon suggest surface extension occurred during lower lithospheric contraction after heat production (U, Th) declined within the PKT ~ 4.0–3.0 Ga (Andrews-Hanna et al., 2014). The gravity anomalies are interpreted to be a network of lava-flooded rift valleys, possibly coinciding with the onset of high-density, extrusive mare volcanism (~3.9 Ga, Hiesinger et al., 2010). Note also, the density of KREEP basalt 15386 (~2700 kg/m^3) is similar to the density of the theoretical Mg-suite parent compositions explored here (Fig. 1). However, crystallization ages for KREEP basalts place them just prior to or contemporaneous with a predominance of mare basaltic volcanism (e.g., Nyquist and Shih, 1992), suggesting low-density, KREEP volcanism may also be related to the rifting event proposed by Andrews-Hanna et al. (2014).

Ancient cryptomare deposits detected remotely and mare clasts such as meteorite Kalahari 009 (~4.3 Ga) may indicate volcanic eruptions occurred contemporaneously with Mg-suite intrusive

magmatism (>4.1 Ga) (e.g., Taylor et al., 1983; Nyquist and Shih, 1992; Terada et al., 2007; Whitten and Head 2015a, 2015b). As discussed above, other factors may have contributed to the eruption of ancient magmas. For example, the hydrostatic ascent model predicts that a deeper source region (the term is used here to also define the region where melts can pond to form a pre-eruptive reservoir) will result in more excess positive pressure at the LNB, possibly explaining the presence of high-density mare basalts at the surface (e.g., Solomon, 1975; Wilson and Head, 1981). When applying the hydrostatic ascent model to the Mg-suite however, eruptions are expected to occur for Mg-suite source depths >20 km, implying an extremely shallow source region of melting and/or that buoyancy forces primarily controlled Mg-suite melt transport (Prissel et al., 2013).

Prior to the recent update of crustal densities from the Gravity Recovery and Interior Laboratory (GRAIL) mission, Wieczorek et al. (2001) investigated the distribution of basaltic volcanism on the Moon as a function of magmatic buoyancy and impact processes. The authors suggest mare magmas with densities greater than upper crustal densities erupt only when the upper anorthositic crust (LNB) is removed via impact excavation. With some caveats, this model can predict the global distribution of younger mare basaltic volcanism on the Moon. Wieczorek et al. (2001) also show that mare melts ascending at super-liquidus temperatures would have lower bulk densities and thus, be more capable of erupting.

Finally, the exsolution of dissolved volatiles from an ascending magma can aid in driving extrusive volcanism, specifically fire fountain eruptions (Wilson and Head, 1981, Fogel and Rutherford 1995; Nicholis and Rutherford 2009, Rutherford and Papale, 2009). For example, lunar picritic glass beads are coated with several volatile elements (C, S, Na, K, Cl, F, P, etc.) suggesting they erupted within a vapor cloud (e.g. Nicholis and Rutherford, 2009, Rutherford and Papale, 2009). Furthermore, dissolved volatile species as well as gas bubbles lower the bulk density of an ascending magma and may contribute to rapid propagation of an intruding dyke tip, perhaps leading to basaltic eruptions (e.g., Wilson and Head, 2007). As a corollary, this may indicate Mg-suite parental melts were nominally anhydrous and/or the Mg-suite source region was volatile-depleted.

5. Conclusions

Results from this study suggest Mg-suite parental melts were capable of erupting only within a few regions of the lunar surface (< 10% globally). The Mg-suite plagioclase-undersaturated melt is the highest density Mg-suite melt considered (2757 kg/m^3) and thus, the most likely to remain intrusive relative to the other Mg-suite parental melts. Because of its likelihood to remain intrusive, the Mg-suite plagioclase-undersaturated parental melt is consistent with the current sample set and petrogenetic models, which suggest the Mg-suite was predominantly intrusive.

The potential regions of eruption predicted for alternative Mg-suite melts are focused within the nearside southern highlands and South Pole-Aitken basin. The presence of remotely observed Mg-suite related rocks (PSA) within the southern highlands region of the Moon suggests this is the most promising area for investigation of ancient, Mg-suite extrusive volcanism. Mg-suite volcanic deposits may be buried by impact ejecta or younger basalt flows. If so, Mg-suite extrusive deposits may be detected in a similar manner to cryptomare via the presence of dark haloed craters (e.g., Whitten and Head, 2015a, 2015b) or as positive Bouguer anomolies in gravity and topography data (e.g., Jozwiak et al., 2012, 2015; Thorey et al., 2015; Sori et al., 2016). Thus, low-density, low-FeO Mg-suite basaltic compositions (in addition to high-density, high-FeO mare compositions) should be included in future remote sensing studies aimed at characterizing igneous mafic material, particularly in the nearside southern highlands region of the Moon.

The low average crustal densities measured by GRAIL are consistent with the apparent lack of Mg-suite volcanic activity. This implies present day fractures of the lunar crust were acquired shortly after primary crustal genesis creating a porous, low-density megaregolith that acted as a barrier to Mg-suite eruptions. A network of lava-filled rift valleys bordering the PKT may indicate extensional stresses occurred ~4.0–3.0 Ga, possibly explaining the presence of younger, high-density mare (and low-density KREEP) basaltic volcanism. Additional factors such as hydrostatic forces, impact-removal of a LNB within the crust, and dissolved volatile species may also contribute to both ancient and younger basaltic volcanism.

Acknowledgments

We would like to thank and greatly appreciate Mark Wieczorek and the GRAIL team for the gravity data used in this study. We also extend a special thank you to both Brad Jolliff for fruitful conversations and Oded Aharonson for serving as our editor. This manuscript benefited from the insightful reviews of Larry Taylor, Satoru Yamamoto, and one unnamed reviewer. This research was supported through the NASA SSERVI Grant NNA14AB01A.

Supplementary materials

Supplementary material associated with this article can be found, in the online version, at doi:10.1016/j.icarus.2016.05.018.

References

Andrews-Hanna, J.C., Asmar, S.W., Head III, J.W., et al., 2013. Ancient igneous intrusions and early expansion of the Moon revealed by GRAIL. Science 339 (6120), 675–678.

Andrews-Hanna, J.C., Besserer, J., Head III, J.W., et al., 2014. Structure and evolution of the lunar procellarum region as revealed by GRAIL gravity data. Nature 514. doi:10.1038/nature13697.

Arai, T., Takeda, H., Miyamoto, M., et al., 2006. Apollo 14 oldest mare basalt revisited: possible petrogenetic connection between Mg gabbronorite and VHK basalt. In: Proceedings of the 37th Lunar Planet Science Conference.

Besserer, J., Nimmo, F., Wieczorek, M.A., et al., 2014. GRAIL gravity constraints on the vertical and lateral density structure of the lunar crust. Geophys. Res. Lett. 41, 5771–5777.

Borg, L., Connelly, J., Cassata, W., et al., 2013. Evidence for widespread magmatic activity at 4.36 Ga in the lunar highlands from young ages determined on troctolite 76535. In: Proceedings of the 44th Lunar Planet Science Conference.

Bottinga, Y., Weill, D.F., 1972. The viscosity of magmatic silicate liquids. A model calculation. Am. J. Sci. 272, 438–475.

Cahill, J.T.S., Lucey, P.G., Wieczorek, M.A., 2009. Compositional variations of the lunar crust: Results from radiative transfer modeling of central peak spectra. J. Geophys. Res.: Planets 114 (E9), E09001. doi:10.1029/2008JE003282, org.

Carlson, R.W., Borg, L.E., Gaffney, A.M., et al., 2014. Rb-Sr, Sm-Nd and Lu-Hf isotope systematics of the lunar Mg-suite: Refining the age and duration of lunar crust formation. Philos. Trans. R. Soc. A 372. doi:10.1098/rsta.2013.0246.

Cheek, L.C., Pieters, C.M., 2014. Reflectance spectroscopy of plagioclase-dominated mineral mixtures: Implications for characterizing lunar anorthosites remotely. Am. Mineral. 99, 1871–1892.

Chin, G., Brylow, S., Foote, M., et al., 2007. Lunar reconnaissance orbiter overview: The instrument suite and mission. Space Sci. Rev. 129, 391–419.

Delano, J.W., 1986. Pristine lunar glasses: Criteria, data, and implications. J. Geophys. Res. 91 (B4), 201–213.

Delano, J.W., 1990. Buoyancy-driven melt segregation in the Earth's Moon, I. Numerical results. In: Proceedings of the 20th Lunar Planet Science Conference, pp. 3–12.

Dhingra, D., Pieters, C.M., Boardman, J.W., et al., 2011. Compositional diversity at Theophilus crater: Understanding the geological context of Mg-spinel bearing central peaks. Geophys. Res. Lett. 38 (11). doi:10.1029/2011GL047314.

Elardo, S.M., Draper, D.S., Shearer, C.K., 2011. Lunar magma ocean crystallization revisited: Bulk composition, early cumulate mineralogy, and the source regions of the highlands Mg-suite. Geochim. Cosmochim. Acta 75, 3024–3045.

Finnila, A.B., Hess, P.C., Rutherford, M.J., 1994. Assimilation by lunar mare basalts: Melting of crustal material and dissolution of anorthite. J. Geophys. Res. 99 (E7), 14677–14690.

Fogel, R.A., Rutherford, M.J., 1995. Magmatic volatiles in primitive lunar glasses: I. FTIR and EPMA analyses of Apollo 15 green and yellow glasses and revision of the volatile-assisted fire-fountain theory. Geochim. Cosmochim. Acta 59 (1), 201–215.
Ghiorso, M.S., Kress, V.C., 2004. An Equation of state for silicate melts II. Calibration of volumetric properties at 10^5 Pa. Am. J. Sci. 304, 679–751.
Giguere, T.A., Hawke, B.R., Taylor, P.G., et al., 1998. Geochemical studies of lunar cyrptomare, Abstract#1782. In: Proceedings of Lunar and Planetary Science Conference, LPSC XXIX.
Gross, J., Treiman, A.H., 2011. Unique spinel-rich lithology in lunar meteorite ALHA 81005: Origin and possible connection to M3 observations of the farside highlands. J. Geophys. Res. 116 (E10). doi:10.1029/2011JE003858.
Han, S., Schmerr, N., Neumann, G., et al., 2014. Global characteristics of porosity and density stratification within the lunar crust from GRAIL gravity and lunar orbiter laser altimeter topography data. Geophys. Res. Lett. 41, 1882–1889. doi:10.1002/2014GL059378.
Haskin, L.A., Gillis, J.J., Korotev, R.L., et al., 2000. The materials of the lunar procellarum KREEP terrane: A synthesis of data from geomorphological mapping, remote sensing, and sample analyses. J. Geophys. Res. 105, 20403–20415.
Hauri, E.H., Saal, A.E., Rutherford, M.J., et al., 2015. Water in the Moon's interior: Truth and consequences. Earth Planet. Sci. Lett. 409, 252–264.
Hawke, B.R., Bell, J.F., 1981. Remote sensing studies of lunar dark-halo impact craters: Preliminary results and implications for early volcansim. In: Proceedings of Lunar and Planetary Science Conference, 12B, pp. 665–678.
Hawke, B.R., Giguere, T.A., Blewett, D.T., et al., 2002. Igneous activity in the southern highlands of the Moon. J. Geophys. Res. 107, 5122. doi:10.1029/2000JE001494, No. E12.
Head, J.W., 1976. Lunar volcanism through space and time. Rev. Geophys. Space Phys. 14 (2), 265–300.
Head, J.W., Wilson, L., 1992. Lunar mare volcanism: Stratigraphy, eruption conditions, and the evolution of secondary crusts. Geochim. Cosmochim. Acta 56 (6), 2155–2175.
Hess, P.C., 1994. Petrogenesis of lunar troctolites. J. Geophys. Res. 99 (E9), 19083–19093.
Hess, P.C., Parmentier, E.M., 1995. A model for the thermal and chemical evolution of the Moon's interior: implications for the onset of mare volcanism. Earth Planet. Sci. Lett. 134 (3–4), 501–514.
Hiesinger, H, Head III, J.W., Wolf, U., et al., 2010. Ages and stratigraphy of lunar mare basalts in Mare Frigoris and other nearside maria based on crater size-frequency distribution measurements. J. Geophys. Res. 115 (E3). doi:10.1029/2009JE003380.
Huppert, H.E., Sparks, R.S.J., 1988. The generation of granitic magmas by intrusion of basalt into continental crust. J. Petrol. 29 (3), 599–624.
Jackson, C.R.M., Cheek, L.C., Williams, K.B., 2014. Visible-infrared spectral properties of iron-bearing aluminate spinel under lunar-like redox conditions. Am. Mineral. 99 (10), 1821–1833.
James, O.B., Hedenquist, J.W., 1978. Spinel-bearing troctolitic basalt 73215,170: Texture, mineralogy, and history. In: Proceedings of the 9th Lunar and Planetary Science Conference, pp. 588–590.
James, O.B., 1980. Rocks of the early lunar crust.. In: Proceedings of the 11th Lunar and Planetary Science Conference, pp. 365–393.
Jessberger, E.K., 1979. Ancient pink-spinel-bearing troctolitic basalt in Apollo 17 Breccia 73215. In: Proceedings of the 10th Lunar and Planetary Science Conference, pp. 625–627.
Jolliff, B.L., Gillis, J.J., Haskin, L.A., et al., 2000. Major lunar crustal terranes: Surface expressions and crust-mantle origins. J. Geophys. Res. 105, 4197–4216.
Jozwiak, L.M., Head, J.W., Zuber, M.T., et al., 2012. Lunar floor-fractured craters: Classification, distribution, origin and implications for magmatism and shallow crustal structure. J. Geophys. Res. 117, E11. doi:10.1029/2012JE004134.
Jozwiak, L.M., Head, J.W., Wilson, L., 2015. Lunar floor-fractured craters as magmatic intrusions: Geometry, modes of emplacement, associated tectonic and volcanic features, and implications for gravity anomolies. Icarus 248, 424–447.
Kramer, G.Y, Kring, D.A., Nahm, A.L., et al., 2013. Spectral and photogeologic mapping of Schrodinger Basin and implications for post-South\sPole-Aitken impact deep subsurface stratigraphy. Icarus 223, 131–148.
Kress, V.C., Carmichael, I.S.E., 1991. The compressibility of silicate liquids containing Fe_2O_3 and the effect of composition, temperature, oxygen fugacity and pressure on their redox states. Contrib. Mineral. Petrol. 108, 82–92.
Lange, R.L., Carmichael, I.S.E., 1987. Densities of Na_2O–K_2O–CaO–MgO–FeO–Fe_2O_3–Al_2O_3–TiO_2–SiO_2 liquids: New measurements and derived partial molar properties. Geochim. Cosmochim. Acta 51, 2931–2946.
Lange, R.L., Carmichael, I.S.E., 1990. Thermodynamic properties of silicate liquids with emphasis on density, thermal expansion and compressibility. Rev. Mineral. Geochem. 24, 25–64.
Longhi, J., Durand, S.R., Walker, D., 2010. The pattern of Ni and Co abundances in lunar olivines. Geochim. Cosmochim. Acta 74, 784–798.
Lister, J.R., Kerr, R.C., 1991. Fluid-mechanical models of crack propagation and their application to magma transport in dykes. J. Geophys. Res. 96 (B6) 10,049-10,077.
Lucey, P.G., Cahill, J.T.S., 2009. The composition of the lunar surface relative to lunar samples. In: Proceedings of the 40th Lunar and Planetary Science Conference.
Michaut, C., 2011. Dynamics of magmatic intrusions in the upper crust: Theory and applications to laccoliths on Earth and the Moon. J. Geophys. Res. 116, B05205. doi:10.1029/2010JB008108.
Morgan, Z., Liang, Y., Hess, P., et al., 2006. An experimental study of anorthosite dissolution in lunar picritic magmas: implications for crustal assimilation processes. Geochim. Cosmochim. Acta 70 (13), 3477–3491.
Norman, M.D., Ryder, G., 1979. A summary of the petrology and geochemistry of pristine highlands rocks. In: Proceedings of the 10th Lunar and Planetary Science Conference, pp. 531–559.
Nicholis, M.G., Rutherford, M.J., 2009. Graphite oxidation in the Apollo 17 orange glass magma: implications for the generation of a lunar volcanic gas phase. Geochim. Cosmochim. Acta 73 (19), 5905–5917.
Nyquist, L., Shih, C.-Y., 1992. The isotopic record of lunar volcanism. Geochim. Cosmochim. Acta 56 (6), 2213–2234.
Papike, J.J., Hodges, F.N., Bence, A.E., et al., 1976. Mare basalts: Crystal chemistry, mineralogy, and petrology. Rev. Geophys. Space Phys. 14 (4), 475–540.
Papike, J.J., Fowler, G.W., Shearer, C.K., et al., 1996. Ion microprobe investigation of plagioclase and orthopyroxene from lunar Mg-suite norites: Implications for calculating parental melt REE concentrations and for assessing post-crystallization REE redistribution. Geochim. Cosmochim. Acta 60, 3967–3978.
Papike, J.J., Ryder, G., Shearer, C.K., 1998. Lunar samples. Rev. Mineral. 36, 5-1–5-234.
Pieters, C.M., Besse, S., Boardman, J., et al., 2011. Mg-spinel lithology: A new rock type on the lunar farside. J. Geophys. Res. 116 (E6). doi:10.1029/2010JE003727.
Pieters, C.M., Hanna, K.D., Cheek, L., et al., 2014. The distribution of Mg-spinels across the Moon and constraints on crustal origin. Am. Mineral. 99 (10), 1893–1910. doi:10.2138/am-2014-4776.
Prissel, T.C., Parman, S.W., Jackson, C.R.M., et al., 2012. Melt–wallrock reactions on the Moon: Experimental con- straints on the formation of newly discovered Mg-spinel anorthosites. In: Proceedings of the 43rd Lunar and Planetary Science Conference.
Prissel, T.C., Parman, S.W., Head, J.W., et al., 2013. Mg-suite plutons: Implications for mantle-derived magma source depths on the Moon. In: Proceedings of the 44th Lunar and Planetary Science Conference.
Prissel, T.C., Parman, S.W., Jackson, C.R.M., et al., 2014. Pink Moon: The petrogenesis of pink spinel anorthosites and implications concerning Mg-suite magmatism. Earth Planet. Sci. Lett. 403, 144–156.
Prissel, T.C., Whitten, J.L., Parman, S.W., et al., 2015. Buoyancy driven magmatic ascent of Mg-suite parental melts. In: Proceedings of the 46th Lunar and Planetary Science Conference.
Prissel, T.C., Parman, S.W., Head, J.W., 2016. Formation of the lunar highlands Mg-suite as told by spinel. Am. Mineral. 101. doi:10.2138/am-2016-5581.
Rubin, A.M., 1993. Dikes vs. diapirs in viscoelastic rock. Earth Planet. Sci. Lett. 117, 653–670.
Rubin, A.M., 1995. Propagation of magma-filled cracks. Annu. Rev. Earth Planet. Sci. 23, 287–336.
Rutherford, M.J., Tonks, B., Holmberg, B., et al., 1996. Experimental study of KREEP basalt evolution: The origin of QMD and granite at the base of the lunar crust. #1113. In: Proceedings of the 27th Lunar and Planetary Science Conference.
Rutherford, M.J., Papale, P., 2009. Origin of basalt fire-fountain eruptions on Earth versus the Moon. Geology 37, 219–222.
Ryder, G., 1991. Lunar ferroan anorthosites and mare basalt sources: The mixed connection. Geophys. Res. Lett. 18, 2065–2068.
Ryder, G., 1994. Coincidence in time of the Imbrium Basin impact and Apollo 15 KREEP volcanic flows: The case for impact-induced melting. Geol. Soc. Am. 293, 11–18.
Saal, A.E., Hauri, E.H., Casicio, M.L., et al., 2008. Volatile content of lunar volcanic glasses and the presence of water in the Moon's Interior. Nature. 454. doi:10.1038/nature07047.
Schultz, P.H., Spudis, P.D., 1979. Evidence for ancient lunar basalts. In: Proceedings of Lunar and Planetary Science Conference, 10, pp. 2899–2918.
Scott, D.H., 1972. Geologic map of the maurolycus quadrangle of the Moon. U.S. Geol. Survey Misc. Geol. Inv. Map I-695.
Shannon, R.D., Prewitt, C.T., 1969. Effective ionic radii in oxides and fluorides. Acta Cryst. B25, 925–946.
Shaw, H.R., 1972. Viscosities of magmatic silicate liquids: An empirical method of prediction. Am. J. Sci. 272, 870–893.
Shearer, C.K., Papike, J.J., 1999. Magmatic evolution of the Moon. Am. Mineral. 84, 1469–1494.
Shearer, C.K., Papike, J.J., 2005. Early crustal building processes on the moon: Models for the petrogenesis of the magnesian suite. Geochim. Cosmochim. Acta 69, 3445–3461.
Shearer, C.K., Hess, P.C., Wieczorek, M.A., et al., 2006. Magmatic and thermal history of the Moon. Rev. Min. Geochem. 60, 365–518.
Shearer, C.K., Burger, P.V., Guan, Y., 2012. Post-LMO crustal growth. A comparison of Apollo 17 dunites. In: Proceedings of the 2nd Conference on Lunar Highlands Crust.
Shearer, C.K., Elardo, S.M., Petro, N.E., et al., 2015. Origin of the lunar highlands Mg-suite: An integrated petrology, geochemistry, chronology, and remote sensing perspective. Am. Mineral 100, 294–325. doi:10.2138/am-2015-4817.
Smith, D.E., Zuber, M.T., Jackson, G.B., et al., 2010. The lunar orbiter laser altimeter investigation on the lunar reconnaissance orbiter mission. Space Sci. Rev. 150, 209–241.
Snyder, G.A., Neal, C.R., Taylor, L.A., 1995. Processes involved in the formation of magnesian-suite plutonic rocks from the highlands of the Earth's Moon. J. Geophys. Res. 100, 9388–9635.
Snyder, G.A., Taylor, L.A., Halliday, A., 1995. Chronology and petrogenesis of the lunar highlands alkali suite: Cumulates from KREEP basalt crystallization. Geochim. Cosmochim. Acta 59, 1185–1203.

Snyder, G.A., Taylor, L.A., Patchen, A., et al., 1999. Mineralogy and Petrology of a Primitive spinel troctolite and gabbros from luna 20, eastern highlands of the Moon. In: Proceedings of the 30th Lunar and Planetary Science Conference.
Solomon, S.C., 1975. Mare volcanism and lunar crustal structure. In: Proceedings of Lunar and Planetary Science Conference, 6, pp. 1021–1042.
Sonzogni, Y., Treiman, A.H., 2015. Parent magma compositions of lunar highlands Mg-suite rocks: A melt inclusion perspective. In: Proceedings of the 46th Lunar and Planetary Science Conference.
Sori, M.M., Zuber, M.T., Head, J.W., et al., 2016. Gravitational search for cryptovolcanism on the Moon: Evidence for large volumes of early igneous activity. Icarus 273. doi:10.1016/j.icarus.2016.02.009.
Taylor, L.A., Shervais, J.W., Hunter, R.H., et al., 1983. Pre-4.2 AE mare-basalt volcanism in the lunar highlands. Earth Planet. Sci. Lett. 66, 33–47.
Taylor, L.A., Lu, F., 1992. The formation of ore mineral deposits on the Moon: A feasibility study. In: Proceedings of the 2nd Conference on Lunar Bases and Space Activities of the 21st Century, 2, pp. 379–383.
Taylor, G.J., 2009. Ancient lunar crust: Origin, composition, and implications. Elements 5, 17–22.
Tekada, H., Yamaguchi, A., Bogard, D.D., et al., 2006. Magnesian anorthosites and a deep crustal rock from the farside crust of the Moon. Earth Planet. Sci. Lett. 247, 171–184.
Terada, K., Anand, M., Soko, A.K., et al., 2007. Cryptomare magmatism 4.35 Gyr ago recorded in lunar meteorite Kalahari 009. Nature 450, 849–852. doi:10.1038/nature06356.
Thorey, C., Michaut, C., Wieczorek, M., 2015. Gravitational signatures of lunar floor-fractured craters. Earth Planet. Sci. Lett. 424, 269–279.
Tompkins, S., Pieters, C.M., 1999. Mineralogy of the lunar crust: Results from clementine. Meteorit. Planet. Sci. 34 (1), 25–41.
Treiman, A.H., Gross, J., 2013. Basalt related to lunar Mg-suite plutonic rocks: A fragment in lunar meteorite ALH81005. In: Proceedings of the 76th Annual Meteorological Society Meeting.
Treiman, A.H., Gross, J., 2015. A rock fragment related to the magnesian suite in lunar meteorite Allan Hills (ALHA) 81005. Am. Mineral. 100, 414–426.
Walker, D., Kirkpatrick, R.J., Longhi, J., et al., 1976. Crystallization history of lunar picritic basalt sample 12002 – Phase-equilibria and cooling-rate studies. Geol. Soc. Am. Bull. 87, 646–656.
Warren, P.H., 1986. Anorthosite assimilation and the origin of the Mg/Fe-related bimodality of pristine moon rocks: Support for the magmasphere hypothesis. J. Geophys. Res. 91 (B4), 331–343.
Warren, P.H., 1988. The origin of pristine KREEP: Effects of mixing between urKREEP and the magmas parental to the Mg-rich cumulates. In: Proceedings of Lunar and Planetary Science Conference, 18, pp. 233–241.
Whitten, J.L., Head, J.W., 2015a. Lunar cryptomaria: Physical characteristics, distribution, and implications for ancient volcanism. Icarus 247, 150–171.
Whitten, J.L., Head, J.W., 2015b. Lunar Cryptomaria: Mineralogy and composition of ancient volcanic deposits. Planet. Space Sci doi:10.1016/j.pss.2014.11.027.
Williams, K.B., Jackson, C., Cheek, L., et al., 2012. The effect of Cr content on the reflectance properties of Mg- spinel, Abstract P43A-1905. In: Am. Geophys.
Williams, K.B., Jackson, C.R.M., Cheek, L.C., et al., 2016. Reflectance spectroscopy of chromium-bearing spinel with application to recent orbital data from the Moon. Am. Mineral. 101, 726–734.
Wilson, L., Head, J.W., 1981. Ascent and eruption of basaltic magma on the Earth and Moon. J. Geophys. Res 86 (B4), 2971–3001.
Wilson, L., Head, J.W., 2007. An integrated model of kimberlite ascent. Nature 447. doi:10.1038/nature05692.
Wieczorek, M.A., Phillips, R.J., 2000. The “Procellarum KREEP Terrane”: Implications for mare volcanism and lunar evolution. J. Geophys. Res. 105, 20417–20430.
Wieczorek, M.A., Zuber, M.T., Phillips, R.J., 2001. The role of magma buoyancy on the eruption of lunar basalts. Earth Planet. Sci. Lett. 185, 71–83.
Wieczorek, M.A., Neumann, G.A., Nimmo, F., et al., 2013. The crust of the Moon as seen by GRAIL. Science 339 (6120), 671–675.
Wood, J.A., Dickey Jr., J.S., Marvin, U.B., et al., 1970. Lunar anor- thosites and a geophysical model of the Moon. Proceedings of the Apollo 11 Lunar Science Conference, Vol. 1, pp. 965–988.
Xu, Y., Zhu, D., Wang, S., 2014. Constraints on volatile concentrations of pre-eruptive lunar magma. Phys. Earth Planet. Int. 229, 55–60.
Yamamoto, S, Nakamura, R., Matsunaga, T., et al., 2012a. Olivine-rich exposures in the South Pole-Aitken Basin. Icarus 218, 331–334.
Yamamoto, S, Nakamura, R., Matsunaga, T., et al., 2012b. Massive layer of pure anorthosite on the Moon. Geophys. Res. Lett. 39, L13201. doi:10.1029/2012GL052098.
Yamamoto, S, Nakamura, R., Matsunaga, T., et al., 2015. Global occurrence trend of high-Ca pyroxene on lunar highlands and its implications. J. Geophys. Res. 120, 831–848.